

# *In Vitro* and *In Cellulo* Anti-Diabetic Activity of Au<sup>I</sup>- and Au<sup>III</sup>-Isothiourea Complexes

Sharmeen Fayyaz<sup>a</sup>, Muniza Shaikh<sup>a</sup>, Danila Gasperini<sup>b</sup>, Steven P. Nolan<sup>c</sup>, Andrew D. Smith<sup>b</sup>, and M. Iqbal Choudhary<sup>\*a, d</sup>

<sup>a</sup>*Dr. Panjwani Center for Molecular Medicine and Drug Research, International Center for Chemical and Biological Sciences, University of Karachi, Karachi-75270, Pakistan*

<sup>b</sup>*EaStCHEM, School of Chemistry, University of St Andrews, St Andrews, Fife, KY16 9ST, UK*

<sup>c</sup>*Department of Chemistry, Ghent University, Krijgslaan 281, S3, Ghent 9000 Belgium*

<sup>d</sup>*Department of Chemistry, Faculty of Science and Technology, Universitas Airlangga, Komplek Campus C, Surabaya 60115, Indonesia*

## **Abstract:**

Gold complexes are known for different biological activities. Considering this precedent, and growing interest in developing metal-based enzyme inhibitors, we report here the dipeptidyl peptidase-IV (DPP-IV) inhibitory potential of cationic, and neutral chiral gold (I), and gold (III) isothiourea complexes. Colorimetric assay with recombinant DPP-IV enzyme was employed for initial screening. Kinetic based mechanistic studies were also performed for most active complexes. Efficiency of identified inhibitors in biological environment was assessed in *in cellulo* assay, using Caco-2 cell line. These complexes showed a good to moderate inhibition of DPP-IV with IC<sub>50</sub> values in the range of 22.0 – 99.0 μM, as compared to standard inhibitor sitagliptin (IC<sub>50</sub> = 0.033 ± 0.04 μM). It was observed that steric, and electronic properties of the isothiourea ligands have profound effect on the DPP-IV inhibitory activity of these complexes. To the best of our knowledge this study reports for the first time on isothiourea based gold complexes for the inhibition of DPP-IV enzyme. These results thus provide an approach for exploring new insights into the development of effective agents against diabetes using incretin-based therapy.

**Key words:** Gold complexes; Dipeptidyl peptidase-IV; Diabetes type 2; Caco-2 cells; Isothiourea; Bioinorganic chemistry

27 Type II diabetes mellitus (T2DM) is termed as “disease of millenia”. It is the most prevailing  
28 disease worldwide. According to an estimation of the World Health Organization (WHO), 300  
29 million people will suffer from diabetes in 2025 [1]. This alarming increase in the prevalence of  
30 diabetes deserves improved and effective strategies for the prevention, and cure of the disease.  
31 Management of diabetes requires a comprehensive and integrated knowledge, and understanding  
32 of various factors involved in the on-set, and progression of the disease. Involvement of multiple  
33 pathophysiological factors in the etiology of disease demands the use of combination therapy in  
34 most of the cases. Therefore, there is a perpetually increasing need of improved anti-diabetic agents,  
35 targeting novel aspects of diabetes [2].

36 Among the hypoglycemic agents, DPP-IV inhibitors are the leading class of oral anti-diabetic  
37 agents. Dipeptidyl peptidase-IV (DPP-IV) is an enzyme responsible for the instant cleavage and  
38 inactivation of incretin (glucose-dependent insulintropic polypeptide (GIP), glucagon-like peptide  
39 1 (GLP-1) hormones. Specific DPP-IV inhibition can lead to an increased half-life of circulating  
40 gut hormones which results in increased insulintropic effect, decrease plasma glucose, and  
41 improves impaired glucose tolerance [3,4]. DPP-IV inhibitors have better safety and tolerability  
42 over other conventional oral anti-diabetic agents. However, adverse effects, such as kidney failure  
43 and pancreatitis, associated with these inhibitors necessitates the development of better treatment  
44 options [5].

45 During the last few years, there have been substantial developments in the field of metallo-drug  
46 discovery. Metal ions and their complexes have been known to play a significant role in various  
47 molecular and cellular processes. Incorporation of metal ions has many advantages over  
48 conventional therapeutic agents [6]. Gold complexes are well known pharmaceuticals [7]. The  
49 unique catalytic properties of gold complexes has attracted the attention of many scientists during  
50 current years, with significant established interest in gold catalysis, and its organometallic  
51 chemistry [8]. Auranofin, a gold (I)-thiolate drug, is used for the treatment of rheumatoid arthritis  
52 [9]. This drug has also been studied as a chemotherapeutic agent against triple negative breast  
53 cancer, and brain tumors [10, 11]. Gold complexes are well known for their role in biological  
54 processes, and are known to possess anti-arthritis [12], anti-cancer [13], anti-bacterial, anti-fungal  
55 [14], anti-leukemia [15], and anti-malarial properties [16]. Isothioureas are widely recognised as  
56 useful organocatalysts, while levamisole (Ergamisol) is a recognised medication used to treat

57 parasitic worm infections [17]. In the present study, we evaluated the DPP-IV inhibitory potential  
58 of isothiourea based gold (I), and gold (III) complexes.

## 59 **2. Experimental**

### 60 **2.1. Material and Methods**

61 All solvents i.e. DMSO (CAS 67-68-5; Scharlau, Spain), and ethanol (CAS 64-17-5; Merck  
62 Millipore, Germany) were of analytical grades, and used without further purification. De-ionized  
63 water was used for buffer preparation. Recombinant human DPP-IV (EC 3.4.14.5) was purchased  
64 from Prof. Dr. Mark D. Gorrell, Sydney, Australia. Tris-(hydroxymethyl)-aminomethane (reagent  
65 grade) was obtained from Merck, Germany. Colorimetric substrate Gly-pro-pNA was obtained  
66 from LeapChem Ltd (Hangzhou, China). Dulbecco's modified eagle medium (DMEM) was  
67 purchased from Caisson Labs, UT, USA.

### 68 **2.2. DPP-IV Enzyme Inhibition Assay**

69 Inhibition of DPP-IV enzyme will be monitored using colorimetric *in vitro* biochemical assay. This  
70 assay involves the cleavage of gly-pro-pNA by enzyme to release *p*-nitroaniline, which gives  
71 absorbance at 400 nm. Initially, 15  $\mu$ L of DPP-IV enzyme (in assay buffer) at the final concentration  
72 of 25 mU/mL was pipetted into a 96-well plate containing test compound to make a final volume  
73 of 50  $\mu$ L. Plate was left for an incubation of 20 min at 37 °C. Reaction was initiated by the addition  
74 of 50  $\mu$ L of substrate dissolved in reaction buffer (Tris-HCl, pH 8.0). Cleavage of substrate by the  
75 DPP-IV enzyme will be monitored at 400 nm using Spectramax M5 (Molecular Devices, CA,  
76 USA). Relative absorbance units per unit of time was converted to the amount of the cleaved  
77 substrate per unit of time ( $\mu$ M/s) by fitting to the calibration curve of free substrate [18].

### 78 **2.3. Assay Protocol for Kinetic Studies**

79 To study different kinetic parameters, activity of enzyme was monitored at various concentrations  
80 of test substances in the presence of different substrate (gly-pro-pNA) concentrations (0.05, 0.1,  
81 0.2, and 0.4 mM) at 400 nm using the same assay protocol as described above. All the experiments  
82 were performed in triplicates. The inhibition pattern was evaluated by Lineweaver–Burk plot,  
83 Dixon plot was constructed between inhibitor concentration [I] and  $1/V_{max}$  to determine the type  
84 of inhibition.  $K_i$  was determined using the curve fitting program, GraFit (Erithacus Software, UK).

## 85 **2.4. *In Cellulo* DPP-IV Activity Assay**

### 86 **2.4.1. Cell Culture**

87 Caco-2 cells (ATCC-HTB37), obtained from ATCC were routinely sub-cultured at 70-80%  
88 confluence, and maintained at 37 °C in a 5% CO<sub>2</sub> atmosphere in high glucose DMEM media  
89 containing 1% non-essential amino acids (GIBCO, Thermo Fisher Scientific, NY, USA),  
90 supplemented with 10% heat-inactivated fetal bovine serum (FBS; Capricorn-Scientific, Germany).

### 91 **2.4.2. *In Situ* Evaluation of the DPP-IV Inhibitory Effect of Gold Complexes**

92 For the experiments, cells were seeded on 96-well plates with clear bottoms at a density of 1 x 10<sup>5</sup>  
93 cells/well. At confluence, spent media was discarded, cells were washed with sterile PBS, and  
94 treated with 50 µL of inhibitor or vehicle in HEPES buffer (20 mM, pH 7.4) for 1 h at 37 °C.  
95 Afterwards 50 µL of the substrate Gly-Pro-pNA (0.2 mM) was added and DPP-IV activity was  
96 recorded using a microplate reader (Molecular Devices, CA, USA) every 1 min for 60 min [19, 20].

## 97 **2.5 Molecular Docking Studies:**

98 The crystal structure of human DPPIV complexed with sitagliptin was downloaded from PDB. The  
99 protein was prepared prior to docking to assign partial charges, adding missing hydrogens and  
100 optimizing the heavy atoms and hydrogen *via* OPLS3e force field [21]. The gold complexes were  
101 sketched and optimized *via* Jaguar module of Maestro, Schrödinger [22]. The grid box on enzyme  
102 was defined by selecting one of the site points on the predicted allosteric binding site. The docking  
103 was carried out in standard precision mode keeping the enzyme rigid and ligands flexible *via*  
104 OPLS3e force-field [23, 24].

105 The docked complexes were further evaluated *via* rescoring with MMGBSA [25] to predict the  
106 binding energies i.e.  $\Delta G_{\text{bind}}$  (Kcal/mol) by using the following equation:

$$107 \Delta G_{\text{bind}} = E_{\text{complex}(\text{minimized})} - E_{\text{ligand}(\text{minimized})} - E_{\text{receptor}(\text{minimized})}$$

108 where,

$$109 E_{\text{complex}(\text{minimized})} = \text{energy of protein–ligand complexes}$$

$$110 E_{\text{ligand}(\text{minimized})} = \text{energy free ligands}$$

$$111 E_{\text{receptor}(\text{minimized})} = \text{energy the free protein}$$

## 2.6 Statistical Analysis

All the experiments were carried out in triplicate, and processed using SoftMax Pro 4.8 software (Molecular Devices, CA, USA). Results are expressed as mean  $\pm$  standard error of mean. IC<sub>50</sub> values were calculated using EZ-FIT enzyme kinetics software (Perrella Scientific Inc., NH, USA).

## 3. Results and Discussion

Isothioureas have been reported as biologically active class of compounds [26]. Heteroatoms in isothiourea structure provide chelating effect, and act as good ligands to facilitate complex formation [27]. There are examples in literature which showed enhanced biological activity of metal complexes as compared to their ligands [28]. Xie *et al* have reported the DPP-IV inhibitory activity of oxidovanadium complexes [29], but there are no reports on anti-diabetic effect of gold complexes targeting DPP-IV. Gasperini *et al.* have recently synthesized a range of novel isothiourea-gold complexes, and reported their biological activities against clinically important enzymes, such as  $\beta$ -glucuronidase, and phosphodiesterase-I. These compounds also showed cytotoxicity against MCF-7, and Hela cancer cell lines [30]. We, therefore, hypothesized that a fundamental study of these gold complexes against dipeptidyl peptidase-IV (DPP-IV) enzyme would be of significant interest for the management of type 2 diabetes mellitus.

### 3.1 *In Vitro* DPP-IV Inhibitory Activity of Gold-complexes

A series of cationic and neutral gold (I), and gold (III) complexes **1–18** were evaluated against human DPP-IV enzyme. These complexes exhibited a good to moderate inhibition of DPP-IV enzyme, with IC<sub>50</sub> values in lower micromolar range (IC<sub>50</sub> = 22.0 - 99.0  $\mu$ M).

Detailed analysis of the DPP-IV inhibitory activity of these ligands indicated that the activity of these complexes is governed by the type of ligand and its absolute configuration, as well as the nature of the counterion. Both the ligand, and counterions play vital roles in the enzyme inhibitory activity of these complexes. Results of the present study are in good accord with the work of Xu *et al.*, which showed that catalytic activity of gold (I) is affected largely by the nature of counterion, and ligands used [31]. During the current study the complexes derived from both enantiomers of two isothiourea Lewis bases, BTM and HyperBTM, were used (Figure-1).

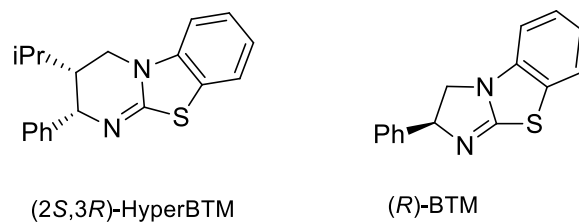


**Figure-1:** Chiral isothioureia ligands used in the study.

The gold complexes evaluated in this study can be divided into the following three classes; cationic gold (I)-isothioureia complexes, neutral gold (I)-isothioureia complexes and gold (III)-isothioureia complexes:

### 3.1.1 Cationic gold (I)-isothioureia complexes

Compounds **1–12** (Figure-2) are cationic gold (I)-isothioureia complexes containing triflimide or tetrafluoroborate counterions. It is widely recognised that changes in structural or electronic properties around the active site of ligands can alter the enzyme inhibitory activities of the precursor metal compounds [32]. We have also observed that complexes coordinated with triphenyl phosphine ( $\text{PPh}_3$ ) showed good enzyme inhibitory activity, as compared to their non-phosphine substituted analogues, such as compounds  $(2R,3S)$ -**1**, and  $(2R,3S)$ -**9** ( $\text{IC}_{50} = 99.0 \pm 0.3$  vs  $59.13 \pm 0.2 \mu\text{M}$ ); and  $(2S,3R)$ -**3**, and  $(2S,3R)$ -**10** ( $\text{IC}_{50} = 66.53 \pm 0.2$  vs  $37.46 \pm 0.1 \mu\text{M}$ ). This effect could be related to  $\pi$ -stacking and cation- $\pi$  interactions between the phenyl phosphane ligand with the enzyme aromatic residues. It is stated in literature that the non-covalent  $\pi$ -stacking, and cation- $\pi$  interactions enhances activity and selectivity [33].

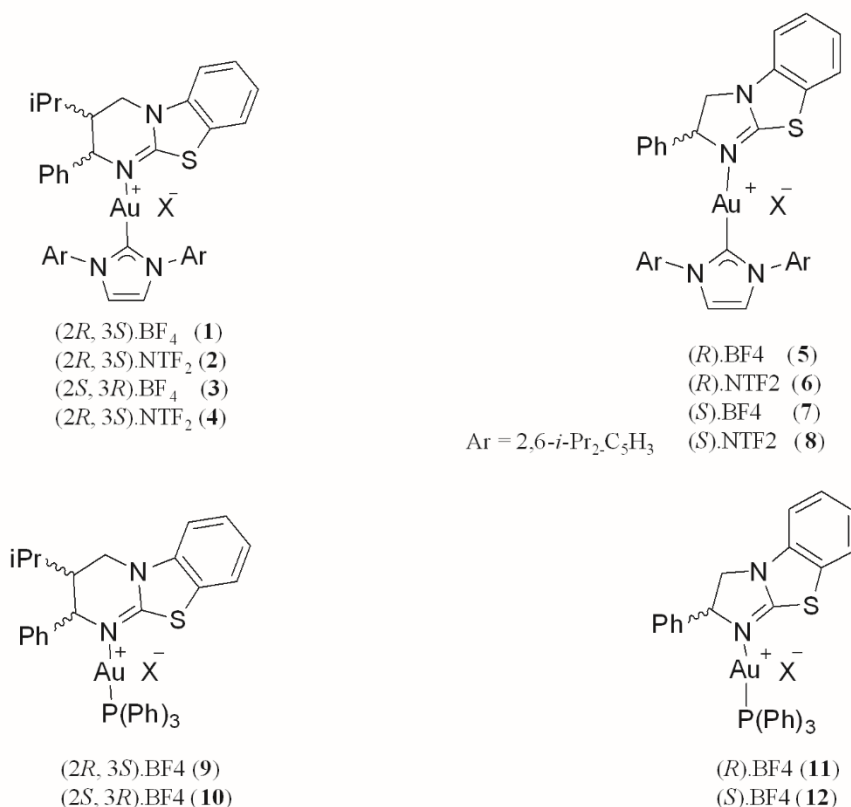
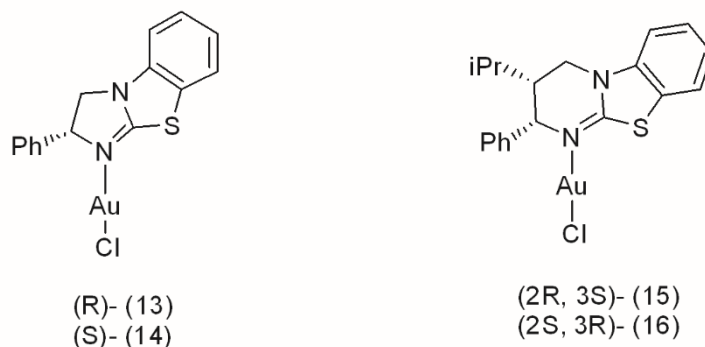


**Figure-2:** Cationic gold (I)-isothioureas complexes used in the study.

156  
 157 Interestingly, complexes (*R*)-**5** and (*R*)-**11**; and (*S*)-**7** and (*S*)-**12**, showed comparable enzyme  
 158 inhibitory activity, indicating that the effect of the ligand (PPh<sub>3</sub> or NHC) is less pronounced when  
 159 (*R*)/(*S*)-BTM was used as Lewis base (IC<sub>50</sub> = 29.88 ± 2.0 and 22.6 ± 0.5; 23.47 ± 0.89 and 35.6 ±  
 160 1.0 μM, respectively). It is worthy to note the different activity of the complexes bearing BTM ((*R*)-  
 161 **5**, (*S*)-**7**, (*R*)-**11** and (*S*)-**12** vs HyperBTM ((2*R*,3*S*)-**1**, (2*S*,3*R*)-**3**, (2*R*,3*S*)-**9** and (2*S*,3*R*)-**10**)  
 162 isothioureas ligands, with the former showing IC<sub>50</sub> lower than 35 μM while the latter being less  
 163 active with IC<sub>50</sub> values higher than 37 μM (Table 1). This effect is presumably related to subtle  
 164 differences in the steric environment associated with HyperBTM compared to the BTM isothioureas.  
 165 It was also observed that the nature of the counterion significantly regulates the DPP-IV inhibitory  
 166 activity of these complexes. Complexes (2*R*,3*S*)-**2**, (2*S*,3*R*)-**4**, (*R*)-**6**, and (*S*)-**8** with the triflimide  
 167 counterion were inactive against DPP-IV enzyme, irrespective of the nature of the Lewis basic  
 168 isothioureas ligand used.

### 3.1.2 Neutral gold (I)-isothioureas complexes

170 Neutral gold (I) complexes **13–16** (Figure-3) were evaluated against DPP-IV enzyme *in vitro*. The  
 171 enantiomeric complexes (*R*)-**13** and (*S*)-**14** bearing BTM ligand showed a good DPP-IV inhibitory  
 172 activity ( $IC_{50} = 45.88 \pm 0.39$ , and  $35.2 \pm 0.9 \mu\text{M}$ , respectively) as compared to HyperBTM  
 173 complexes (*2R,3S*)-**15**, and (*2S,3R*)-**16** with ( $IC_{50} = 81.8 \pm 4.7$  and  $76.9 \pm 3.7 \mu\text{M}$ , respectively).  
 174 This trend is consistent with that observed for the cationic complexes **1 – 12**. Our results are in good  
 175 accord with Inci *et al.*, which suggested that the use of planar aromatic ligands would be of interest  
 176 for the development of efficient DPP-IV inhibitors as anti-diabetic agents [34].



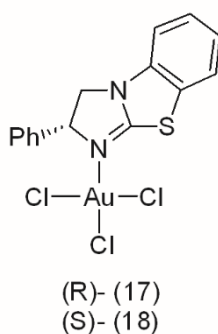
177

178

**Figure-3:** Structures of neutral gold (I) complexes **13 – 16**.

### 179 3.1.3 Gold (III)-isothiourea complexes

180 After the evaluation of series of gold (I) cationic, and neutral chiral gold complexes, DPP-IV  
 181 inhibitory potential of the enantiomeric gold (III) complexes (*R*)-**17** and (*S*)-**18** was investigated  
 182 (Figure-4). Only compound **18** showed a weak enzyme inhibitory activity ( $IC_{50} = 80.5 \pm 1.5 \mu\text{M}$ ).  
 183 The increased Lewis acidity of the  $d^8$  gold (III) center may have resulted in a weak inhibitory effect  
 184 of the complex (Table 1).



185

186

**Figure-4:** Structures of neutral gold (III) complexes.

187



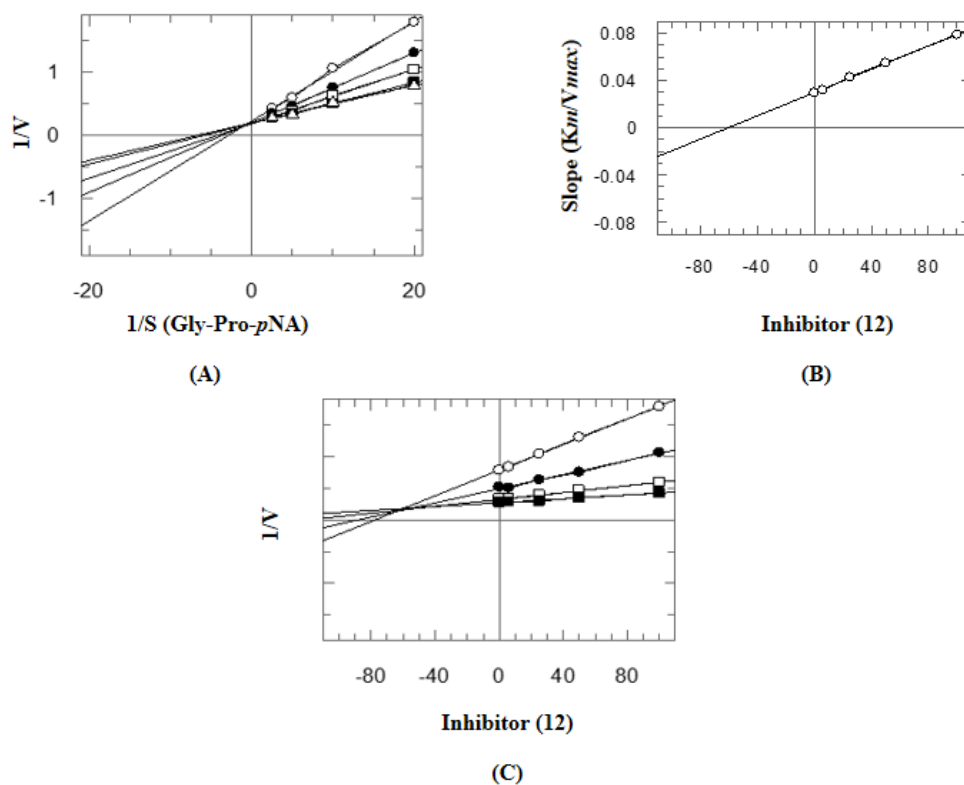
188 **Table 1:** DPP-IV Inhibitory Potential of gold complexes **1-18**.

<b>Compounds</b>	<b>IC<sub>50</sub>± SEM* (µM)</b>	<b>189</b>
<b>Cationic gold (I) complexes</b>		
(2 <i>R</i> ,3 <i>S</i> )- <b>1</b>	99.0 ± 0.3	<del>190</del>
(2 <i>R</i> ,3 <i>S</i> )- <b>2</b>	NA**	191
(2 <i>S</i> ,3 <i>R</i> )- <b>3</b>	66.53 ± 0.2	
(2 <i>S</i> ,3 <i>R</i> )- <b>4</b>	NA	192
( <i>R</i> )- <b>5</b>	29.88 ± 2.0	193
( <i>R</i> )- <b>6</b>	NA	194
( <i>S</i> )- <b>7</b>	23.47 ± 0.89	195
( <i>R</i> )- <b>8</b>	NA	196
(2 <i>R</i> ,3 <i>S</i> )- <b>9</b>	59.13 ± 0.2	197
(2 <i>S</i> ,3 <i>R</i> )- <b>10</b>	37.46 ± 0.1	198
( <i>R</i> )- <b>11</b>	22.6 ± 0.5	199
( <i>S</i> )- <b>12</b>	35.6 ± 1.0	200
<b>Neutral gold (I) complexes</b>		
( <i>R</i> )- <b>13</b>	45.88 ± 0.39	201
( <i>S</i> )- <b>14</b>	35.2 ± 0.9	202
(2 <i>R</i> ,3 <i>S</i> )- <b>15</b>	81.8 ± 4.7	203
(2 <i>S</i> ,3 <i>R</i> )- <b>16</b>	76.9 ± 3.7	204
<b>Gold (III) complexes</b>		
( <i>R</i> )- <b>17</b>	NA	205
( <i>S</i> )- <b>18</b>	80.5 ± 1.5	206

210 \*IC<sub>50</sub> Values are expressed as mean ± S. E. M. (Standard Error of Mean) where n=3; \*\* NA = not active211 **3.2 Mechanistic studies of gold (I) complexes**

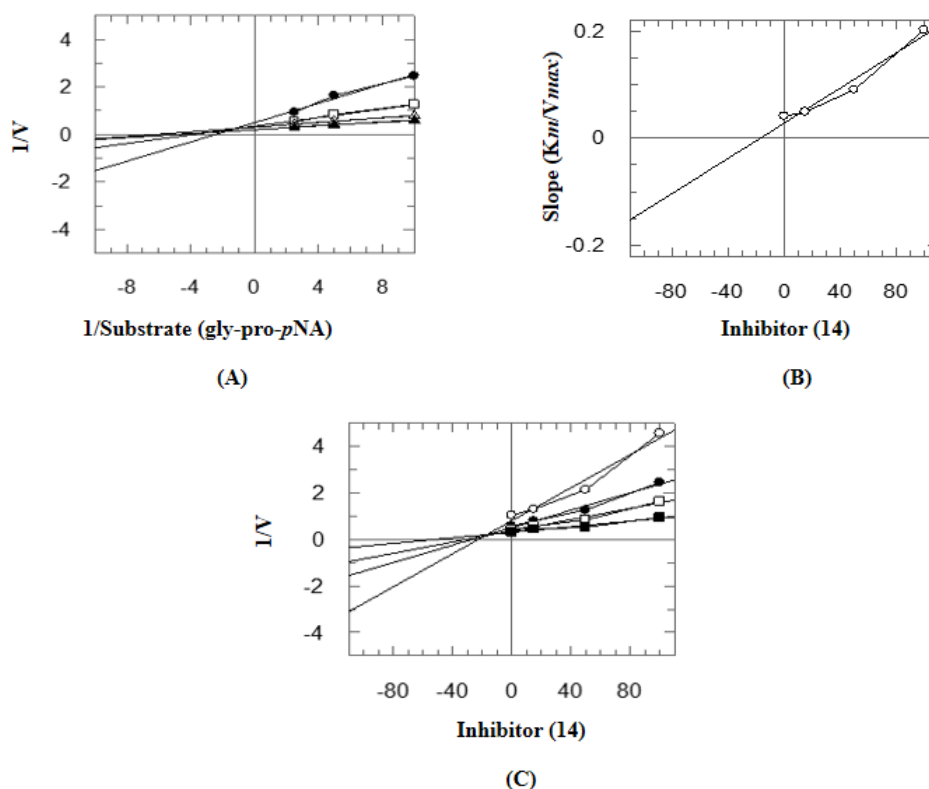
212 The most active cationic, and neutral gold (I) complexes (*R*)-**5**, (*S*)-**7**, (2*S*,3*R*)-**10**, (*R*)-**11**, (*S*)-**12**,  
213 and (*S*)-**14** were subjected to kinetic-based mechanistic studies to identify the type of inhibition.  
214 Mode of inhibition indicated a possible interaction of inhibitors in the active site of enzyme. Kinetic  
215 parameters indicated that complexes (2*S*,3*R*)-**10**, (*R*)-**5**, (*S*)-**7**, and (*S*)-**14** showed non-competitive  
216 type of inhibition, since *K<sub>m</sub>* remains unaffected whereas *V<sub>max</sub>* decreased. Mixed inhibition by  
217 complex (*R*)-**11** was indicated through altered values of both *K<sub>m</sub>* and *V<sub>max</sub>* demonstrate a binding  
218 of this complex with the enzyme at a site other than the substrate binding site with the catalytic  
219 residues of DPP-IV. An increase in the apparent affinity of the enzyme for the substrate (*K<sub>m</sub>*app>  
220 *K<sub>m</sub>*) in the presence of complex (*S*)-**12** was observed, whereas *V<sub>max</sub>* remains unaffected. This  
221 suggests that the inhibitor favours binding with the free enzyme, and inhibits DPP-IV activity in  
222 competitive manner (Table 2). Figure-5, and -6 represents the kinetic graphs for compounds (*S*)-  
223 **12**, and (*S*)-**14** respectively.

224



225 **Figure-5:** Steady state competitive inhibition of DPP-IV enzyme by inhibitor (S)-12. (A) Lineweaver–Burk plot  
 226 between the reciprocal of  $1/V_{max}$  vs  $1/\text{substrate}$  (gly-pro-pNA) in the presence of different concentrations of  
 227 inhibitor,  $I = 100 \mu\text{M}$  ( $\circ$ ),  $I = 50 \mu\text{M}$  ( $\bullet$ ),  $I = 25 \mu\text{M}$  ( $\square$ ),  $I = 6 \mu\text{M}$  ( $\blacksquare$ ), and in the absence of inhibitor,  $I = 0.00 \mu\text{M}$   
 228 ( $\Delta$ ). (B) Secondary re-plot from reciprocal plot for  $K_i$  between slope vs  $[I]$ , (C) Dixon plot, which further confirms  
 229 the  $K_i$ , and type of inhibition, which is competitive for compound (S)-12 against the DPP-IV.

230



232 **Figure-6:** Steady state non-competitive inhibition of enzyme DPP-IV by (*S*)-14. (A) Lineweaver–Burk plot between  
 233 the reciprocal of  $1/V_{max}$  vs  $1/\text{substrate}$  (gly-pro-pNA) in the presence of different concentrations of inhibitor,  $I =$   
 234  $100 \mu\text{M}$  ( $\bullet$ ),  $I = 50 \mu\text{M}$  ( $\square$ ),  $I = 15 \mu\text{M}$  ( $\Delta$ ), and in the absence of inhibitor  $I = 0.00 \mu\text{M}$  ( $\blacktriangle$ ). (B) Secondary re-plot from  
 235 reciprocal plot for  $K_i$  between slope vs  $[I]$ , (C) Dixon plot, which further confirms the  $K_i$ , and type of inhibition,  
 236 which is non-competitive for compound (*S*)-14 against the DPP-IV enzyme.

237

238 **Table 2:** Kinetics parameters for gold complexes.

Compounds	$V_{max}$ ( $\mu\text{M/L/min}$ ) <sup>-1</sup>	$K_m$ (mM)	$V_{max \text{ app}}$ ( $\mu\text{M/L/min}$ ) <sup>-1</sup>	$K_m \text{ app}$ (mM)	$K_i \pm \text{S.E.M.}$ ( $\mu\text{M}$ )	Type of Inhibition
( <i>R</i> )-5	5.88	0.18	4.5	0.19	$42.3 \pm 0.001$	Non-competitive
( <i>S</i> )-7	13.42	0.19	8.92	0.21	$7.18 \pm 0.004$	Non-competitive
(2 <i>S</i> , 3 <i>R</i> )-10	9.35	0.23	16.35	0.19	$35.89 \pm 0.3$	Non-competitive
( <i>R</i> )-11	11.75	0.24	7.45	0.48	$7.4 \pm 0.002$	Mixed

(S)-12	5.03	0.25	4.99	9.8	59.2 ± 0.0002	Competitive
(S)-14	4.9	0.2	2.1	0.28	17.7 ± 0.01	Non-competitive

239

240  $K_m$  = Michaelis-Menten constant in the absence of inhibitor  $K_i$  = dissociation constant of inhibitor,  $K_m$  app = Michaelis-Menten constant in the  
 241 presence of inhibitor,  $V_{max}$  = the maximal velocity at which enzyme show catalysis per unit time,  $V_{max}$  app = the apparent maximal velocity in the  
 242 presence of inhibitor.

243 \* $K_i$  Values are expressed as mean ± S. E. M. (Standard Error of Mean) where n=3

### 244 3.3. *In Cellulo* DPP-IV Inhibition by Gold Complexes

245 Drug development using *in vitro* biochemical assays is often hampered by the lack of *in vivo* activity  
 246 of identified leads due to factors, such as lower intracellular binding selectivity or membrane  
 247 permeability [35]. We, therefore, have evaluated inhibitory potential of cationic, and neutral gold  
 248 (I) complexes against DPP-IV enzyme in Caco-2 cell-based assay. Lower inhibitory potential of  
 249 complexes in *in cellulo* assay, as compared to recombinant DPP-IV enzyme, might be attributed to  
 250 complex biological environment in cellular assay. With the exception of complex (S)-12 which  
 251 showed the maximum inhibitory activity ( $IC_{50} = 20.5 \pm 0.49 \mu M$ ), all other complexes (R)-11, (R)-  
 252 13, and (S)-14 showed comparable inhibition of enzyme DPP-IV *in situ* cellular model, with  $IC_{50}$   
 253 values in the range of 45.8 – 53.6  $\mu M$  (Table 3)

254 **Table 3:** Inhibitory activities of gold complexes in *in situ* Caco-2 DPP-IV inhibition assay.

Compound	$IC_{50} \pm S. E. M^*(\mu M)$
(R)-11	45.8 ± 1.83
(S)-12	20.5 ± 0.49
(R)-13	48.7 ± 5.4
(S)-14	53.6 ± 1.07

255 \* $IC_{50}$  Values are expressed as mean ± S. E. M. (Standard Error of Mean) where n=3

### 256 3.4. Molecular Docking Studies

257 Docking analysis was carried out for selected gold complexes. The compounds in DPP-IV  
 258 inhibitory assay from subclass, cationic gold complexes were chosen *i.e.*, compounds 7, and 11.

259 The crystal structure of DPP-IV complexed with sitagliptin deposited in PDB (PDB ID: 1X70) was  
 260 used for docking analysis. The compounds were docked into the predicted binding site of DPP-IV

261 enzyme obtained *via* site map analysis. The docking score and predictive binding energies are  
262 presented in table 4.

263 **Table 4:** Molecular docking studies of selected gold complexes

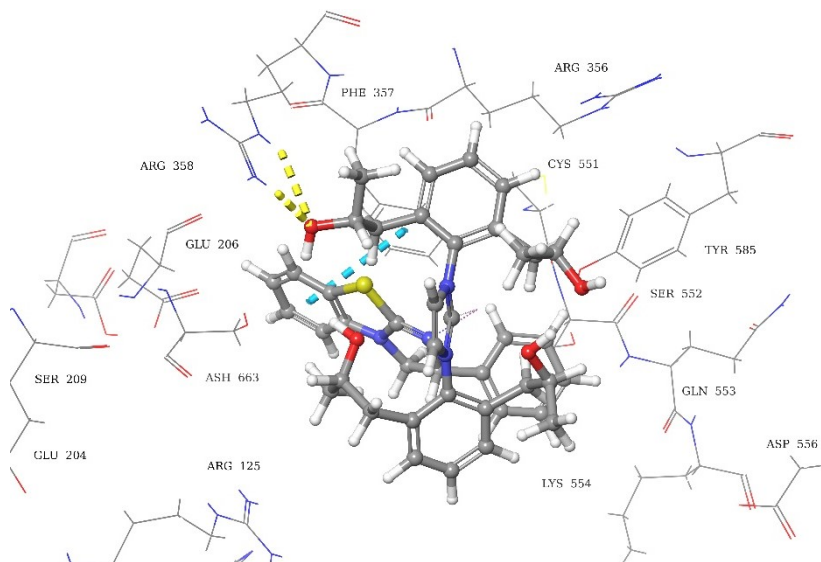
264

Compounds	Docking Score kcal/mol	Predictive binding energy $\Delta G_{\text{bind}}$ kcal/mol
7	-5.3	-56.8
11	-2.9	-16.2

266

267

268 Compound 7 showed hydrogen bonding with Arg 358. While it made  $\pi$ - $\pi$  interaction with Phe 357  
269 (Figure-7). Compound 11 made  $\pi$ -cation interaction with Lys 554 of predicted allosteric site.  
270 (Figure-8).



272 **Figure-7:** 3D ligand interaction diagram of compound 7 in the predicted allosteric site of DPPIV (PDB ID:  
273 1X70). Hydrogen bonding is represented as yellow dashed line.  $\pi$ - $\pi$  Interaction is represented as cyan dotted  
274 lines.

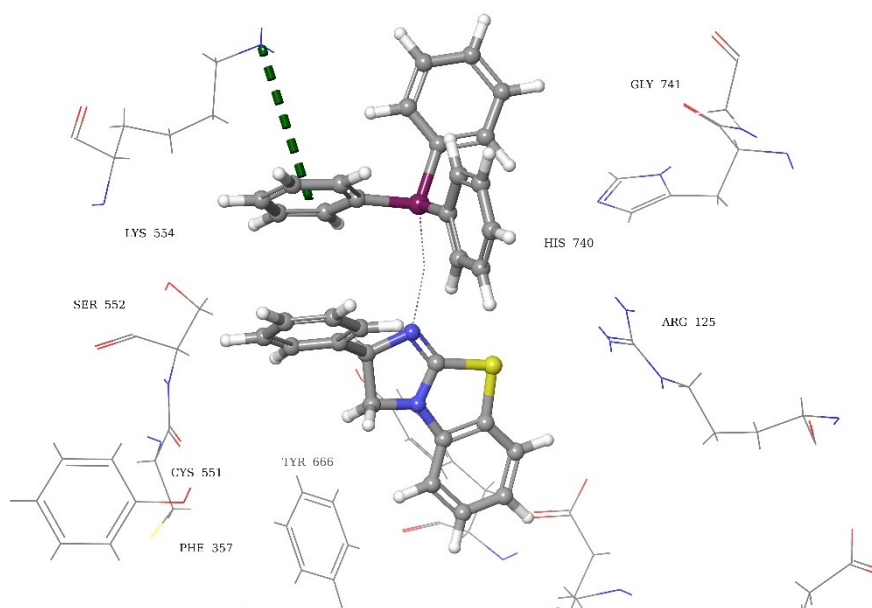


**Figure-8:** 3D ligand interaction diagram of compound **11** in the predicted allosteric site of DPPIV (PDB ID: 1X70). Dotted green line presents the  $\pi$ -cationic interactions.

These preliminary studies have demonstrated the anti-diabetic potential of gold (I), and gold (III)-isothiourea complexes through the inhibition of DPP-IV enzyme *in vitro*. These complexes will serve as leads for the development of DPP-IV inhibitors with improved activity. Our group further continues to investigate the biological interactions of different metal complexes inside the cell to better understand their biochemistry, and mechanism of action.

## Conclusion

During the current study, it was found that both the ligand, and counterion play vital roles in the enzyme inhibitory activity. Triflimide isothiourea gold complexes were found to be inactive, irrespectively of the ligand used, whereas the presence of triphenyl phosphine in isothiourea gold complexes improved the activity. We have identified compound (*S*)-**12** as most promising complex of the series which showed good inhibition in *in cellulo* model. Inhibitory activity of these complexes is modulated by the electronic, and steric effects of the ligands. Moreover, the absolute configuration within the isothiourea might affect the activity of the complexes, with (*S*)-**12** being more active than (*R*)-**11**. Further studies are needed to fully disclose and understand the interactions of the different enantiomers with the enzyme. These results constitute the first report of gold

295 complexes capable of inhibiting DPP-IV in *in vitro*, and *in cellulo* models. Further research is  
296 currently underway to identify the mechanism of action, and to provide complexes with improved  
297 activity for incretin-based therapy.

#### 298 **Acknowledgement**

299 Authors are grateful to the Higher Education Commission (HEC), Pakistan, for providing financial  
300 support under the Indigenous Ph. D. Fellowship for 5000 Scholars Phase-II program for providing  
301 financial support.

#### 302 **4. References**

- 303 1. Kurniawati M, and Mahdi C. The effect of juice mangosteen rind (*Garcinia mangostana* L.)  
304 to blood sugar levels and histological of pancreatic rats with the induction of  
305 streptozotocin. *J Pure Appl Chem Res* 2014;**3**(1):1.
- 306 2. Uddin KN. Insight into newer anti-diabetic treatment. *BIRDEM Med J* 2019;**9**(1):1-6.
- 307 3. Nongonierma AB, Paolella S, Mudgil P, Maqsood S, and FitzGerald RJ. Identification of  
308 novel dipeptidyl peptidase IV (DPP-IV) inhibitory peptides in camel milk protein  
309 hydrolysates. *Food Chem* 2018;**244**:340-348.
- 310 4. Zhang J, Liu Y, Lv J, Cao Y, and Li G. Dipeptidyl peptidase-IV activity assay and inhibitor  
311 screening using a gold nanoparticle-modified gold electrode with an immobilized enzyme  
312 substrate. *Microchim Acta* 2015;**182**(1-2):281-288.
- 313 5. Cai T, Gao Y, Zhang L, Yang T, and Chen Q. Effects of different dosages of Sodium-  
314 Glucose Transporter 2 Inhibitors on lipid levels in patients with type 2 diabetes mellitus: A  
315 protocol for systematic review and meta-analysis. *Medicine*, 2020, **99**(29): e20735.
- 316 6. Banerjee S, Lollar CT, Xiao Z., Fang Y, and Zhou HC. Biomedical Integration of Metal–Organic  
317 Frameworks. *Trends Chem* 2020;**2**(5):467-479
- 318 7. Zhang CX, and Lippard SJ. New metal complexes as potential therapeutics. *Curr Opin Chem*  
319 *Biol.* 2003;**7**(4):481-489.

- 320 8. Amirmahani N, Rashidi M, and Mahmoodi NO. Synthetic application of gold complexes on  
321 magnetic supports. *Applied Organometallic Chemistry. Appl Organomet*  
322 *Chem.* 2020;**34**(5):e5626.
- 323 9. Zoppi C, Messori L, and Pratesi A. ESI MS studies highlight the selective interaction of  
324 Auranofin with protein free thiols. *Dalton Trans.* 2020;**49**(18):5906-5913.
- 325 10. Raninga PV, Lee AC, Sinha D, Shih YY, Mittal D, Makhale A, and Khanna KK. Therapeutic  
326 cooperation between auranofin, a thioredoxin reductase inhibitor and anti-PD-L1 antibody  
327 for treatment of triple-negative breast cancer. *Int J Canc.* 2020;**146**(1):123-136.
- 328 11. Krabbendam IE, Honrath B, Bothof L, Silva-Pavez E, Huerta H, Fajardo NMP, and Kruyt  
329 F. SK Channel activation potentiates auranofin-induced cell death in glio- and neuroblastoma  
330 cells. *Biochem Pharmacol.* 2020;**171**:113714.
- 331 12. Yeo CI, Sim JH, Khoo CH, Goh ZJ, Ang KP, Cheah YK, and Seng HL. Pathogenic Gram-  
332 positive bacteria are highly sensitive to triphenylphosphane-gold (O-alkylthiocarbamates),  
333 Ph<sub>3</sub>PAu [SC (OR)= N (p-tolyl)](R= Me, Et and iPr). *Gold Bull.* 2013; **46**(3):145-152.
- 334 13. Altaf M, Monim-ul-Mehboob M, Kawde AN, Corona G, Larcher R, Ogasawara M, and  
335 Aldinucci D. New bipyridine gold (III) dithiocarbamate-containing complexes exerted a potent  
336 anticancer activity against cisplatin-resistant cancer cells independent of p53 status. *Oncotarget*  
337 2017;**8**(1):490.
- 338 14. Glišić BD, and Djuran MI. Gold complexes as antimicrobial agents: An overview of  
339 different biological activities in relation to the oxidation state of the gold ion and the ligand  
340 structure. *Dalt. Trans.* 2014;**43**(16):5950-5969.
- 341 15. Nunes MS, Garzon LR, Rampelotto RF, Tizotti MK, Martini R, Locatelli A, and Hörner R.  
342 Synthesis, characterization and biological activity of a gold(I) triazenide complex against  
343 chronic myeloid leukemia cells and biofilm producing microorganisms. *Braz J Pharm Sci.*  
344 2017;**53**(4):e00191
- 345 16. Hemmert C, Fabié A, Fabre A, Benoit-Vical F, and Gornitzka H. Synthesis, structures, and  
346 anti-malarial activities of some silver (I), gold (I) and gold (III) complexes involving N-  
347 heterocyclic carbene ligands. *Eur J Med Chem.* 2013;**60**:64-75.



- 348 17. Daniels DSB, Smith SR, Lebl T, Shapland P, and Smith AD. A scalable, chromatography-  
349 free synthesis of benztetramisole. *Synthesis*, 2015;**47**(1):34-41.
- 350 18. Nongonierma AB, Mooney C, Shields DC, and Fitzgerald RJ. Inhibition of dipeptidyl  
351 peptidase IV and xanthine oxidase by amino acids and dipeptides. *Food Chem.* 2013;**141**(1):  
352 644-653.
- 353 19. Brandt I, Joossens J, Chen X, Maes MB, Scharpé S, De Meester I, and Lambeir AM.  
354 Inhibition of dipeptidyl-peptidase IV catalyzed peptide truncation by vildagliptin ((2*S*)-{[(3-  
355 hydroxyadamantan-1-yl) amino] acetyl}-pyrrolidine-2-carbonitrile. *Biochem Pharmacol.*  
356 2005;**70**(1):134-143.
- 357 20. Sadir R, Imberty A, Baleux F, and Lortat-Jacob H. Heparan sulfate/heparin oligosaccharides  
358 protect stromal cell-derived factor-1 (SDF-1)/CXCL12 against proteolysis induced by  
359 CD26/dipeptidyl peptidase IV. *Journal of Biological Chemistry. J Biol Chem.*  
360 **2004**;279(42):43854-43860.
- 361 21. Schrödinger Release 2019-1: Schrödinger Suite 2021-1 Protein Preparation Wizard;  
362 Epik, Schrödinger, LLC, New York, NY, 2021; Impact, Schrödinger, LLC, New York, NY,  
363 2021; Prime, Schrödinger, LLC, New York, NY, 2021.
- 364 22. Schrödinger Release 2021-1: Jaguar, Schrödinger, LLC, New York, NY, 2021
- 365 23. Friesner RA, Banks JL, Murphy RB, Halgren TA, Klicic JJ, Mainz DT, Repasky MP, Knoll  
366 EH, Shaw DE, Shelley M, Perry JK, Francis P, Shenkin PS, Glide: A New Approach for  
367 Rapid, Accurate Docking and Scoring. 1. Method and Assessment of Docking Accuracy. *J*  
368 *Med Chem*, 2004;**47**:1739–1749.
- 369 24. Schrödinger Release 2021-1: Glide, Schrödinger, LLC, New York, NY, 2021.
- 370 25. Schrödinger Release 2021-1: Prime, Schrödinger, LLC, New York, NY, 2021.
- 371 26. Siddiqui N, Alam MS, Sahu M, Naim MJ, Yar MS, and Alam O. Design, synthesis,  
372 anticonvulsant evaluation and docking study of 2-[(6-substituted benzo [d] thiazol-2-  
373 ylcarbamoyl) methyl]-1-(4-substituted phenyl) isothioureas. *Bioorg Chem* 2017;**71**:230-243
- 374 27. Schneider J, Lee Y, Pérez J, Brennessel WW, Flaschenriem C, and Eisenberg R. Strong  
375 intra-and intermolecular aurophilic interactions in a new series of brilliantly luminescent

376 dinuclear cationic and neutral Au (I) benzimidazolethiolate complexes. *Inorg Chem.*  
377 2008;**47**(3):957-968.

378 28. Ashiq U, Jamal RA, Saleem M, and Mahroof-Tahir M. Alpha-glucosidase and carbonic  
379 anhydrase inhibition studies of Pd (II)-hydrazide complexes. *Arab J Chem.* 2017;**10**(4):488-  
380 499.

381 29. Xie MJ, Zhu MR, Lu CM, Jin Y, Gao LH, Li L, Sadler PJ. Synthesis and characterization of  
382 oxidovanadium complexes as enzyme inhibitors targeting dipeptidyl peptidase IV. *J Inorg*  
383 *Biochem.* 2017;**175**:29-35.

384 30. Gasperini D, Greenhalgh MD, Imad R, Siddiqui S, Malik A, Arshad F, Smith AD, and Nolan  
385 SP. Chiral Au<sup>I</sup>- and Au<sup>III</sup>-Isothiourea Complexes: Synthesis, characterization, and  
386 application. *Chem Eur J.* 2019;**25**(4):1064-1075.

387 31. Xu Y, Hu X, Zhang S, Xi X, and Wu Y. Room-temperature hydration of alkynes catalyzed by  
388 different carbene gold complexes and their precursors. *ChemCatChem*, 2016;**8**(1):262-267.

389 32. Renfrew AK. Transition metal complexes with bioactive ligands: mechanisms for selective  
390 ligand release and applications for drug delivery. *Metallomics.* 2014;**6**(8):1324-1335.

391 33. Janardhan S, and Narahari SG. Dipeptidyl peptidase IV inhibitors: a new paradigm in type  
392 2 diabetes treatment. *Curr Drug Targets.* 2014;**15**(6):600-621.

393 34. İnci D, Köşeler A, Zeytünlüoğlu A, Aydın R, and Zorlu Y. Interaction of a new copper (II)  
394 complex by bovine serum albumin and dipeptidyl peptidase-IV. *J Mol Str.* 2019;**1177**:317-  
395 322.

396 35. Luchinat E, Barbieri L, Cremonini M, Nocentini A, Supuran CT, and Banci L. Drug  
397 screening in human cells by NMR spectroscopy allows the early assessment of drug  
398 potency. *Angew Chem Int.* 2013;**59**(16):6535-6539.